



HAL
open science

Trends and inter-annual variability of altimetry-based coastal sea level in the Mediterranean Sea: Comparison with tide gauges and models

H. B. Dieng, A. Cazenave, Y. Gouzenes, B. A. Sow

► **To cite this version:**

H. B. Dieng, A. Cazenave, Y. Gouzenes, B. A. Sow. Trends and inter-annual variability of altimetry-based coastal sea level in the Mediterranean Sea: Comparison with tide gauges and models. *Advances in Space Research*, 2021, 68, pp.3279-3290. 10.1016/j.asr.2021.06.022 . insu-03671324

HAL Id: insu-03671324

<https://insu.hal.science/insu-03671324>

Submitted on 16 Oct 2023

HAL is a multi-disciplinary open access archive for the deposit and dissemination of scientific research documents, whether they are published or not. The documents may come from teaching and research institutions in France or abroad, or from public or private research centers.

L'archive ouverte pluridisciplinaire **HAL**, est destinée au dépôt et à la diffusion de documents scientifiques de niveau recherche, publiés ou non, émanant des établissements d'enseignement et de recherche français ou étrangers, des laboratoires publics ou privés.



Distributed under a Creative Commons Attribution - NonCommercial 4.0 International License

Trends and inter-annual variability of altimetry-based coastal sea level in the Mediterranean Sea: Comparison with tide gauges and models

H.B. Dieng^{1,2,4}, A. Cazenave^{2,3}, Y. Gouzenes² and B.A. Sow⁴

1. OceanNext, 90 CHE DU MOULIN, 38660 LA TERRASSE, France
2. LEGOS: CNRS/CNES/IRD/UT3-PS, 14 Avenue E. Belin, 31400 Toulouse cedex, France
3. International Space Science Institute, Bern, Switzerland
4. Assane Seck University of Ziguinchor, UASZ – Néma II, BP : 523, Ziguinchor, Sénégal.

07 June 2021

Revised
Advances in Space Research

Abstract

In the framework of the Coastal sea level project of the ESA Climate Change Initiative, a new coastal sea level product from the Jason-1, 2 and 3 missions over 2002-2018 has been made recently available. This product consists of along-track, high-resolution (20 Hz, i.e., ~350 m) sea level anomalies and coastal sea level trends derived from a complete reprocessing of the Jason altimetry data, including a retracking of the radar waveforms using the ALES (Adaptive Leading Edge Sub-waveform) retracker, in several coastal regions worldwide. In this study, we extend the assessment of this coastal sea level product in the Mediterranean Sea region by comparing with tide gauge data where available. We selected a set of 14 coastal sites where the distance between the Jason track at the coast is less than 30 km from a tide gauge for which the in-situ record at least partly covers the 2002-present time span. In a first part of this study, we compared the interannual variability and trends of the coastal sea level anomalies and of the tide gauge data. A good agreement is found between the altimetry-based sea level time series and the tide gauge data at interannual time scales. In terms of trends, the comparison also shows general good agreement within the respective uncertainties. In a second part of this study, we focus on the Senetosa site (south Corsica) where a significant altimetry-based sea level trend increase is observed in the last 3-4 km to the coast, and investigate which physical process could explain this trend behavior. We analyzed temperature and salinity data of the high-resolution (400 m) MARS3D model, available around Corsica over the January 2014 - December 2019 time span, and computed the steric sea level component and its trend along the Jason track. A clear steric sea level trend increase is found in the last 3-4 km to the coast. Although the MARS3D model does not provide outputs prior to 2014, we suggest that if the steric sea level trend increase found over 2014-2019 is a long-life time feature, it has the right amplitude to explain the altimetry-based coastal sea level trend increase observed at Senetosa.

1. Introduction

Monitoring coastal zone changes is a major societal issue for the assessment of risks linked to climate change, in particular sea level rise. Sea level variations at the coast have been measured by tide gauges (TG) for many decades, but with a highly non-uniform distribution, both in time and space. Since the early 1990s, high-precision satellite altimetry (e.g. Topex/Poseidon launched in 1992, the Jason series - 1, 2, 3 since 2001, and more recently Sentinel-3A, 3B and Sentinel 6) provide regular monitoring of sea level at global and regional scales. Satellite altimetry indicates that the global mean sea level (GMSL) has increased at a mean rate of 3.3 ± 0.3 mm/yr over the last three decades (Legeais et al., 2018) and even accelerates (Watson et al., 2015, Dieng et al., 2017, Nerem et al., 2018). The GMSL rate of rise is now almost twice the rate reported for the 20th century by TGs (Church et al., 2013, Dangendorf et al., 2017). Satellite altimetry has also shown that sea level rise is non uniform geographically, with rates up to 2-3 times faster than the global mean in some regions. However, because classical altimetry has been optimized for the open ocean, it does not provide accurate information in coastal areas, especially in the first 10-15 km to the coast due to contamination of radar echoes by land surfaces (Cipollini et al., 2017). In the coastal zone, the reflected echoes of classical radar missions may significantly depart from the classical waveform shape observed in the open ocean because of the large radar footprint of most past missions. This makes difficult the estimate of the sea surface height (SSH) measurement. Coastal altimetry measurements are also affected by uncertainties of certain geophysical corrections, in particular the wet troposphere correction, sea state bias, ocean tide and atmospheric loading (Birol et al., 2017). In the recent years, efforts have been developed to improve SSH measurements in coastal areas, either using new altimeter instruments allowing higher along-track resolution, e.g., Ka-band altimetry on SARAL/Altika, or Synthetic Aperture Radar/SAR altimetry on the Sentinel 3A & 3B, and Sentinel-6 Michael Freilich missions, or performing new editing and post-processing techniques of classical altimetry data (Birol et al., 2017) and new retracking methods of the radar waveforms (Passaro et al., 2014). Over the past 15 years, several coastal altimetry products dedicated to coastal studies have been developed. We can quote: (i) the X-TRACK editing tool (Birol et al., 2017) developed by CTOH/LEGOS (Center for Topographic studies on the Ocean and Hydrosphere / Laboratory of Studies in Space Geophysics and Oceanography, France); (ii) ALES (Adaptive Leading Edge Sub-waveform, Passaro et al., 2014) developed by NOC (National Oceanography Center, UK); (iii) PISTACH (Innovative Prototype of a Treatment System for Coastal Altimetry and Hydrology) and its successor PEACHI (Prototype for Expertise on Altimetry for Coastal, Hydrology, and Ice), developed by CLS (Collecte Localisation Satellites, France, Valladeau et al., 2015).

Recently, in the context of the Coastal Sea-Level project (www.esa-sealevel-cci.org/) supported by the Climate Change Initiative (CCI) programme of ESA (European Space Agency), a new coastal sea level product has been derived by a complete reprocessing of Jason-1, 2 and 3 altimetry data, combining the X-TRACK editing tool with the ALES retracking method. This new product provides along-track, high-resolution (20 Hz, i.e., ~ 350 m) sea level anomalies (SLA) over June 2002 to May 2018 (currently extended to December 2019), and associated coastal sea level trends, in six regions

worldwide (The Climate Change Initiative Coastal Sea Level Team, 2020; hereafter noted CSLT2020). Unlike the other coastal products mentioned above, this new coastal sea level dataset provides sea level anomalies (SLAs) and trends up to the last few km to the coast (i.e., largely covering the 10-15 km coastal gap).

In the present study, we extend the tide gauge-based statistical validation made in CSLT2020 through a direct comparison of coastal SLA time series averaged over the first 2 km from the closest valid point from the coast along the track, with tide gauge records in the Mediterranean Sea. Comparison of sea level data from classical altimetry with tide gauge data has been performed for long by several studies, in different regions. For example, along the US coasts (e.g., Salazar-Ceciliano et al., 2018; Ruiz-Etcheverry et al., 2015), in Western Europe (e.g., Gómez-Enri et al., 2018; Fenoglio-Marc et al., 2015), the Mediterranean Sea (e.g., Grgić et al., 2017; Bonnefond et al., 2011), Asia and Australia (e.g., Peng and Deng, 2018; Idris et al., 2017) and West Africa (e.g., Dieng et al., 2019; Angnuureng et al., 2018). However, the present study is the first to consider high-resolution (350 m), reprocessed sea level data in the coastal zones of the Mediterranean Sea. A set of 14 TGs records are available at distances less than 30 km from the Jason tracks. Some of the tide gauges have a GNSS station nearby, allowing in principle to correct the TG records for vertical land motions (VLMs). But in general, the period covered by the GNSS data do not overlap with the time span considered here, so that except in one case, VLMs are corrected for the Glacial Isostatic Adjustment (GIA) only. We also considered, for comparison, gridded sea level data from classical altimetry (the CMEMS/DT2018 dataset) as well an ocean reanalysis (the CMEMS MED-Physics model).

2. Data and method

2.1. Altimetry data

For the altimeter-based sea level data, we use two different products: (1) the ESA CCI Coastal Sea Level product and (2) the gridded data from Copernicus Marine Environment Monitoring Service (CMEMS).

2.1.1. The CCI Coastal sea level product

The CCI coastal sea level product (called Coastal Sea Level Product 2'; The Climate Change Coastal Sea Level Team, 2020) is publicly available from the SEANOE website: <https://doi.org/10.17882/74354>. It consists of along-track SLA data at 20 Hz (i.e., a distance of ~350 m between two successive points along the Jason track) and monthly resolution, reprocessed using the X-TRACK/ALES system. It nominally covers June 2002 - May 2018, but is currently extended up to December 2019. Detailed information on the processing methodology, geophysical corrections and editing process can be found in Marti et al. (2019), Gouzenes et al. (2020), CSLT2020 and Birol et al. (2021).

The ‘Coastal Sea Level Product 2’ provides a total of 70 sites in the Mediterranean Sea. However, as indicated in the introduction, only 14 are located nearby a tide gauge. The nominal study period considered here is January 2002 to December 2018 (we do not consider year 2019 because some other data are not available beyond December 2018).

2.1.2 CMEMS/DT2018 : Altimetry gridded data

We also considered the CMEMS/DT2018 gridded data (level 4) version (<http://marine.copernicus.eu/>), available over the period 1993-2019 (Taburet et al., 2019). The gridded data are based on a large set of altimetry missions (repeated track, geodetic and new interleaved orbits) merged together (Taburet et al., 2019). The gridded SLA data are provided daily on a $0.25^\circ \times 0.25^\circ$ grid over 82°N and 82°S latitudinal range. .

2.2. Tide gauge data

The TG data come from the August 2020 version of the Permanent Service for Mean Sea Level (PSMSL) database (<https://www.psmsl.org/>). We used monthly data (Holgate et al., 2013; PSMSL, 2018) from 14 stations along the coasts of the Mediterranean Sea, located less than 30 km from the first valid point of the altimetry tracks (see Fig.1 showing the positions of the TGs and the Jason tracks). Some of the TGs have some missing data over our study period January 2002 – December 2018. Considering the missing data on the time series of some of the TG after 2015, we compared the coastal sea level products over 3 different time spans: January 2002 – December 2018, January 2002 - December 2016 and January 2002 – December 2015, depending on the TG data availability. For the comparison with altimetry-based SLAs, the TG data need to be corrected for vertical land motions (VLMs). Five tide gauges (out of 14) have a GNSS station nearby (at less than 10 km distance; e.g., Imperia, Eze, Sete, Trieste and Senetosa), but except for Senetosa, the other four GNSS time series only partially cover our study period, with data length of a few years only. Besides, in several cases, the VLMs based on the solutions of different GNSS data centers (SONEL/University of La Rochelle, Nevada Geodetic Laboratory, GFZ and JPL) display trend differences larger than the quoted uncertainties. Therefore we decided not to use the GNSS-based VLMs (except for Senetosa) but only correct for the GIA-related VLM using the gridded ICE5Gv1.3_VM2 model from Peltier (2004) (available from the PSMSL web site).

2.4. Numerical models

2.4.1. CMEMS MED-Physics ocean reanalysis

We considered The CMEMS MED-Physics product (https://doi.org/10.25423/MEDSEA_REANALYSIS_PHYS_006_004), developed by the Mediterranean Forecasting System and distributed by CMEMS (<http://marine.copernicus.eu/>). This is an oceanic physical reanalysis that uses a hydrodynamic model provided by the Nucleus for European Modeling of the Ocean (NEMO), with a variational data assimilation scheme (OceanVAR) for

temperature and salinity vertical profiles and satellite SLA along-track data (Simoncelli et al., 2019). This product provides gridded monthly SSH data for the period January 1987 to December 2018 with horizontal resolution of $1/16^\circ$ (approximately 6 -7 km). The model covers the entire Mediterranean Basin.

2.4.2 MARS3D numerical model

MARS3D (Model for Applications at Regional Scales) is a numerical community model with 3-spatial-dimensions (3D) developed by IFREMER (Institut Français de Recherche pour l'Exploitation de la Mer) and distributed by the DYNECO/DHYSED team (HYdro-SEDimentaire Dynamics laboratory of the DYNamics of Coastal Ecosystems department, <http://wwz.ifremer.fr/dyneco/Lab.-Dhysed>). This model is dedicated to coastal oceanography, from regional scales (a few tens of km) to coastal scales (a few hundred meters) (Lazure and Dumas, 2008).

In this study, we used bathymetry, temperature and salinity gridded data from the MARS3D model, with a spatial resolution of about 400 m. However, the simulation is not available throughout the whole Mediterranean Sea but only in the region around Corsica (40.72°N - 43.31°N ; 8.15°E - 9.94°E).

2.5 Post processing of the data

A number of post processings were applied to the data:

(1) Each time series was corrected for its time average. It is equivalent to applying an additional offset to each chosen sea level time series so that their mean value is zero (Risien and Strub, 2016; Idris et al., 2017 and Dieng et al., 2019). Note that removing the mean from sea level does not affect the calculation of the trend, but only the variability.

(2) The SLAs and tide gauge data are already provided at monthly interval. Since we are interested here in the interannual variability, we removed the annual and semi-annual signals by fitting sinusoidal functions to the SLA time series, and further applied a 3-month moving average shifted by 1 month.

(3) To be homogeneous with the SLA data already corrected for atmospheric loading (see, The Coastal Sea Level Team, 2020), the tide gauge data have been corrected for the inverted barometer (IB) using surface pressure data from the ERA Interim reanalysis from ECMWF (Dee et al., 2011;

<https://www.ecmwf.int/en/forecasts/datasets/reanalysis-datasets/era-interim>). For that purpose, we interpolated the gridded pressure data at the tide gauge position.

(4) Because some tide gauge records suffer data gaps, we applied an optimal interpolation of the 'Spline' type to cover the missing temporal data, notably those greater than 3 months. This is a continuous second derivative interpolator that can represent peaks quite well. We compared this method ('Spline') with a standard linear interpolation and found a better estimate of the sea level trend with errors reduced by more than 10% especially when the SLA presents temporal holes of more than 6 month (this is the case for several TGs). In short, the 'Spline' method best preserves time series trends and adapts to rapid changes in gradient or slope. (5) The altimetry SLAs time series were also compared to the gridded CMEMS/DT2018 altimetry-data set and to the CMEMS MED-Physics ocean reanalysis.

For that purpose, we considered the gridded data located on the circle whose center is the point of the Jason track. Considering the resolution of the CMEMS/DT2018 and CMEMS MED-Physics grids, circle radii of 25 km and 10 km were considered respectively.

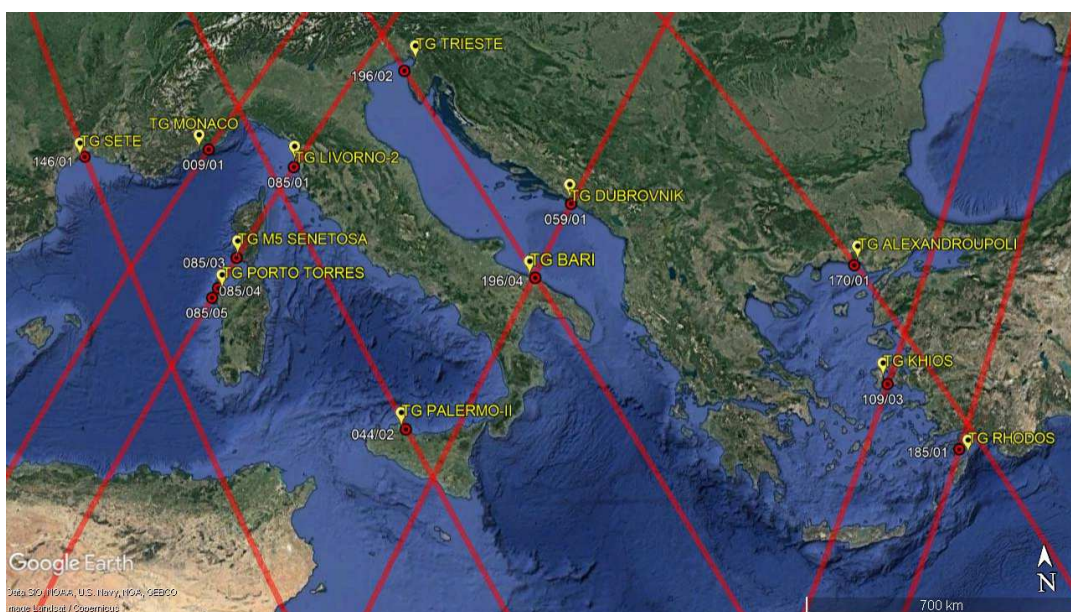
(6) For each time series, trend and associated 1-sigma formal error were estimated through a least-squares fit of a linear function. Note that we have not corrected the altimetry SLAs for the glacial isostatic adjustment (GIA) because its value is low (<0.4 mm/yr; Peltier, 2004) in the Mediterranean Sea.

3. Comparison of altimetry-based coastal sea level anomalies (SLA) and tide gauges data

3.1 Method

As indicated in the introduction, the main objective of this study is to compare SLAs time series (focusing on interannual variability) and trends with sea level time series from nearby tide gauges in the Mediterranean Sea. This extends the validation already performed in the study by CSLT2020 in which the validation with tide gauges was performed via a statistical approach. In the latter study, altimetry-based SLAs were not taken at the closest point from a tide gauge but at some along-track point nearby where the altimetry time series showed the highest correlation with the tide gauge record. Because this method was applied to the 429 sites of the ‘Coastal Sea Level Product 2’, no detailed information was given on the distance to the tide gauge of the selected along-track altimetry time series. Here, we follow a different (but complementary) approach that consists of averaging successive 20 Hz SLAs along the Jason track, over a distance of 2 km in the offshore direction from the closest valid point to the coast. This spatially averaged time series will be the one compared to the nearby tide gauge record.

From the 66 portions of tracks selected in CSLT2020 for the Mediterranean Sea, we considered only those located within 30 km of a tide gauge. This led us to keep only 14 track portions. Fig.1 shows the



location of the 14 track portion and the tide gauges.

Fig.1: Google Earth image of the Mediterranean Sea with the selected Jason tracks (red lines) and tide gauge sites (yellow symbols). The red circles represent the altimetry-based coastal sites and the numbers indicate the site number on the Jason track.

Table 1 gathers the names and coordinates of the tide gauges, the time span they cover as well as the distance to the altimetry coast point (2 km average) and associated Jason track number.

Table 1: List of altimetric sites with a tide gauge (TG) available within 30 km of the point where the Jason track crosses land. Also indicated in the table, the coordinates (latitude, longitude) of the first along-track valid point from coast, and its distance to the coast. The tide gauge names and coordinates and time span of data availability are also given.

Track/site	First SLA valid point coordinates : Latitude(°N) longitude (°E)	Distance of the altimetry first point to the coast (km)	Tide gauge name	Tide gauge coordinates: Latitude(°N) longitude (°E)	Tide gauge record period	Distance of altimetry first point to closest tide gauge (km)
009/01	43.77 7.74	2.77	MONACO	43.73 7.42	1956-2018	25.6
044/02	38.13 13.50	1.33	PALERMO-II	38.12 13.37	2001-2015	11.7
059/01	42.60 18.12	2.55	DUBROVNIK	42.66 18.06	1956-2018	7.9
085/01	43.46 10.31	2.36	LIVORNO-II	43.55 10.30	2001-2015	9.9
085/03	41.55 8.79	1.13	SENETOSA M5	41.56 8.80	2001-2019	1.3
085/04	40.91 8.31	4.82	PORTO TORRES	40.84 8.40	2001-2015	10.7
085/05	40.68 8.14	4.38	PORTO TORRES	40.84 8.40	2001-2015	28.6
109/03	38.25 26.27	1.41	KHIOS	38.37 26.14	1969-2015	17.4
146/01	43.45 3.87	3.49	SETE	43.40 3.70	1960-2018	15.3
170/01	40.79	6.24	ALEXANDROUPOLIS	40.84	1969-2018	8.9

	25.80			25.88		
185/01	36.55 27.99	0.83	RHODOS & RHODOS-II	36.44 28.24	1969-2016	24.8
196/02	45.47 13.46	3.14	TRIESTE	45.65 13.76	1975-2019	30.0
196/04	41.14 17.04	5.61	BARI	41.14 16.87	2001-2015	14.4
222/02	40.94 8.68	2.61	PORTO TORRES	40.84 8.40	2001-2015	25.7

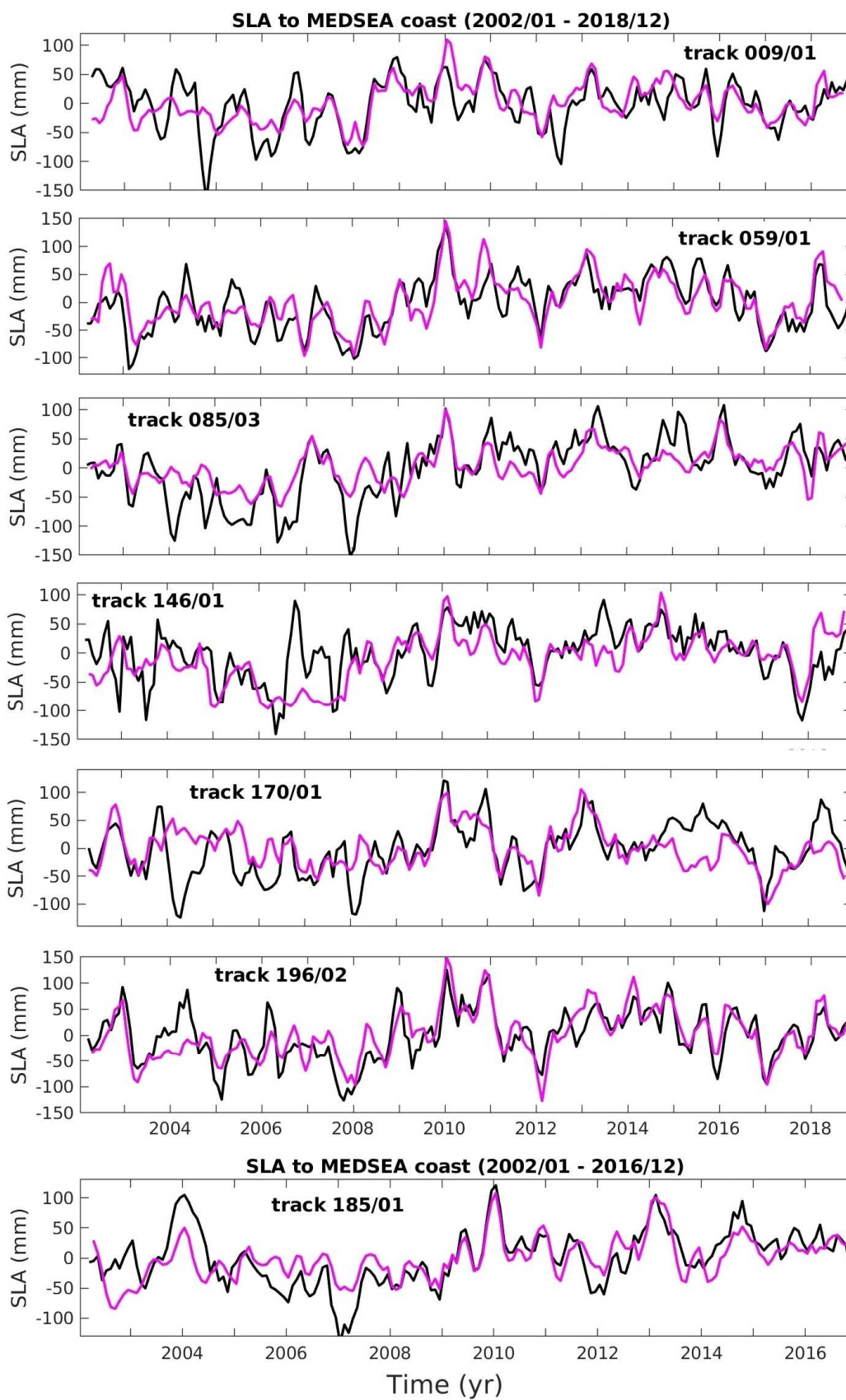
The altimetry SLAs time series were also compared to the gridded CMEMS/DT2018 altimetry-data set and to the CMEMS MED-Physics ocean reanalysis. For that purpose, we considered the gridded data located on the circle whose center is the point of the Jason track. Considering the resolution of the CMEMS/DT2018 and CMEMS MED-Physics grids, circle radii of 25 km and 10 km were considered respectively.

For each time series, trend and associated 1-sigma formal error were estimated through a least-squares fit of a linear function. Note that we have not corrected the altimetry SLAs for the glacial isostatic adjustment (GIA) because its value is low (<0.4 mm/yr; Peltier, 2004) in the Mediterranean Sea.

3.2 Results

3.2.1 Interannual variability

Fig. 2 shows the altimetry time series superimposed to the tide gauge records at each of the 14 selected tracks. Six time series cover the period 2002-2018 (Jason tracks numbers 009/01, 059/01, 085/03, 146/01, 170/01 and 196/02), one covers the 2002-2016 period (Jason track number 185/01) and eight cover the 2002-2015 time span (Jason track numbers 009/01bis, 044/02, 085/01, 085/04, 085/05, 109/03, 196/04 and 222/02).



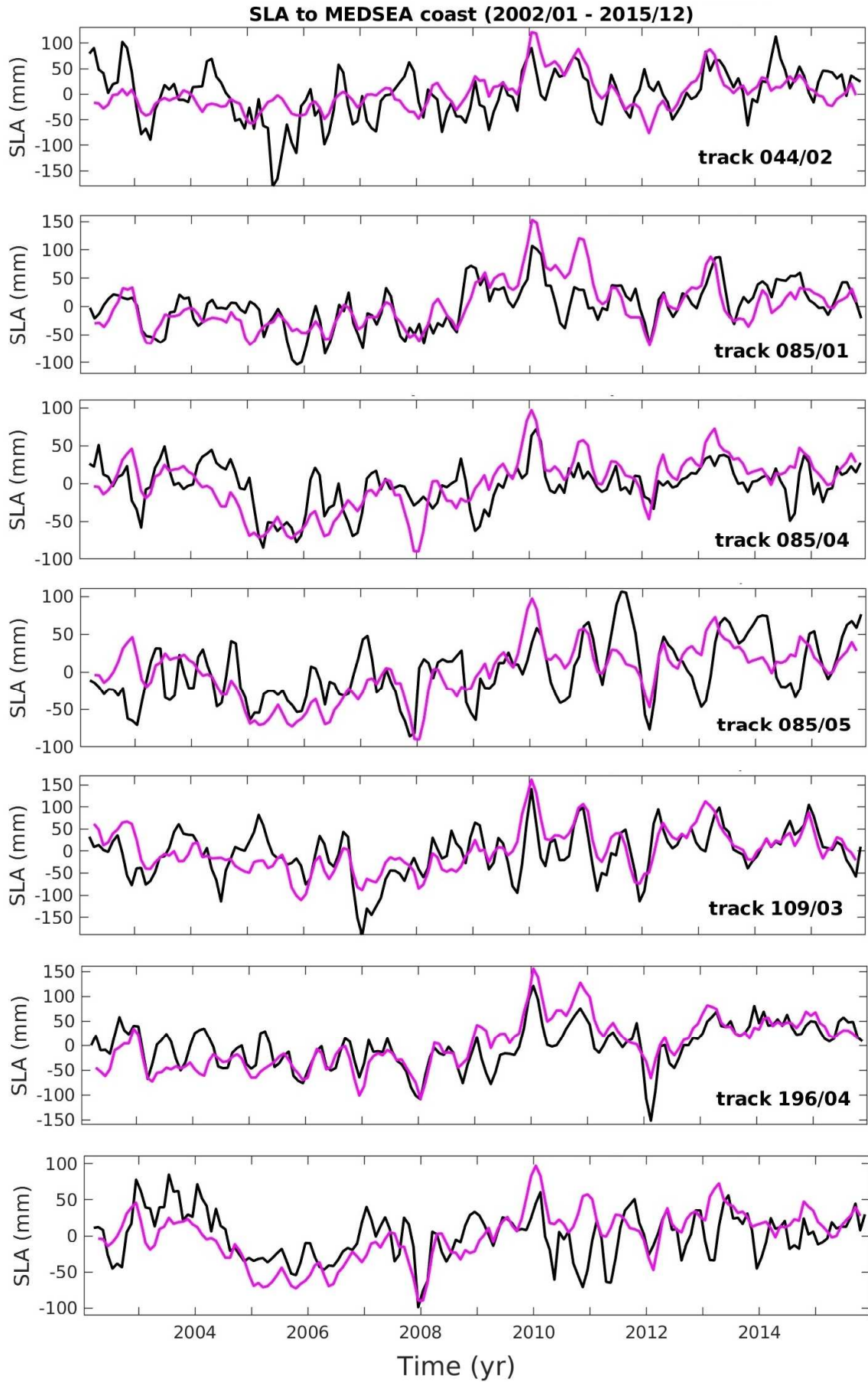


Fig.2 : Coastal SLA time series (2 km averages; black) and tide gauge records (purple) at the 14 selected sites. (a) for tracks 9/1, 59/1, 85/3, 146/1, 170/1, 196/2 and 185/1. (b) for

tracks 44/2, 85/1, 85/4, 85/5, 196/2 and 222/2.

Table 2 gathers the root-mean-squares (RMS) differences between altimetry-based coastal sea level time series and tide gauge records, as well as the correlation between the two time series.

Table 2. RMS differences (upper number) and correlation (lower number) between tide gauge (TG) sea level time series and altimetry-based coastal, CMEMS/DT2018 and CMEMS/Med-Physics model time series. The distance between the TG and the altimetry-based along-track coastal sea level point is also indicated (last column)

Jason track	Tide gauge sea level versus Altimetry-based coastal RMS (mm) <u>Correlation (in bold)</u>	Tide gauge sea level versus CMEMS/DT2018 RMS (mm) <u>Correlation (in bold)</u>	Tide gauge sea level versus CMEMS MED-Physics model RMS (mm) <u>Correlation (in bold)</u>	Distance Altimetry-TG (km)
2002/01-2018/12				
009/01	35 0.60	25 0.63	25 0.66	25.9
059/01	31 0.77	24 0.87	27 0.77	7.8
085/03	35 0.72	19 0.78	29 0.43	1.3
146/01	40 0.55	32 0.68	34 0.61	15.3
170/01	39 0.54	21 0.84	30 0.73	8.9
196/02	32 0.80	25 0.89	27 0.82	30
2002/01-2016/12				
185/01	33 0.70	26 0.72	30 0.60	24.8
2002/01-2015/12				
044/02	46 0.43	18 0.85	24 0.69	11.7
085/01	33 0.69	25 0.85	31 0.67	9.9
085/04	30 0.60	23 0.81	28 0.49	10.7

085/05	39 0.48	23 0.80	28 0.47	28.7
109/03	46 0.60	21 0.91	26 0.85	17.4
196/04	34 0.73	27 0.92	28 0.72	14.4
222/02	35 0.52	22 0.84	28 0.52	25.7

We note satisfactory agreement between altimetry and tide gauge time series at the 14 studied sites. This agreement is particularly good at some sites, where the correlation is > 0.7 . This is the case for tracks 059/01, 85/3, 185/01, 196/2 and 196/04. The effect of the distance between the tide gauge and satellite track (closest valid point to the coast) has no significant impact on the comparison. For example, the best correlation (0.8) corresponds to a distance of 30 km between tide gauge and Jason track.

The RMS of the difference time series (altimetry minus tide gauge) are in the range 30–45 mm, with a mean value of 36 mm. This value is to be compared to the average square-root variance of the signal, on the order of 100 mm (or slightly larger).

Table 2 also shows the RMS and correlation between TGs and gridded CMEMS/DT2018 and CMEMS/Med-Physics model time series. In the case of the CMEMS/DT2018, the correlation is quite high and slightly larger than for the coastal SLAs. This may suggest that either the coastal SLAs are noisier than open ocean data or that they capture some local oceanic signal not active offshore nor seen by the tide gauges (which are in general located in sheltered zones at the coast). More likely, this reflects a larger noise level of the coastal data. The comparison with the model data shows much variation from one site to another, but high correlation and low RMS at several sites.

We also analyzed the effects of spatial and temporal smoothing of SLAs. We considered 3 cases: (1) monthly data with 3-month smoothing and spatial average over 2 km for X-TRACK/ALES data (as in Table 2); (2) monthly data without smoothing and spatial average over 2 km, and (3) monthly data with 3-month smoothing and spatial average over 4 km. We note that the temporal smoothing allows a significant improvement of the statistics (an improvement $\sim 20\%$ for the correlation and $\sim 44\%$ for the RMS). On the other hand, spatial smoothing contributes only $\sim 3\%$ for the improvement of correlation and $\sim 14\%$ in terms of RMS. This suggests that the high-frequency signal (from one month to another) mostly contributes to the RMS.

3.2.2 .Trends

We estimated the trends of the coastal altimetry and tide gauge time series over their overlapping time spans. As mentioned above, we did not correct the tide gauge data for the GNSS-based VLM because

available GNSS data do not overlap the full observational period of the tide gauge records, except at Senetosa where a GNSS time series covers the full time span. Thus to account for the VLMs, we only corrected for GIA using the gridded ICE5Gv1.3_VM2 model from Peltier (2004).

Altimetry-based coastal and tide gauge trends are presented in Table 3. SLA trends from CMEMS/DT2018 and CMEMS MED-Physics model (considering the grid point closest to the coast) are also shown.

Table 3: Coastal sea level trends (mm/yr) for the four different products (SLAs, tide gauges/TG, CMEMS/DT2018 and CMEMS MED-Physics model over 3 different periods (2002/01 – 2018/12 ; 2002/01 – 2016/12 ; 2002/01- 2015/12). The VLM trend is corrected for in the TG series, using either the GIA model or the GNSS solution (latter case indicated by *).

Jason track	Distance between Jason track and TG (km)	TG trend (mm/yr)	TG trend after correcting for VLM using either the GIA model or the GNSS* trend	Altimetry-based coastal trend (average over 2 km from first valid point) mm/yr	CMEMS/DT2018 trend (mm/yr)	CMEMS MED-Physics model trend (mm/yr)
2002/01-2018/12						
009/01	25.85	1.75 ± 0.47	1.76 ± 0.47	0.95 ± 0.64	2.54 ± 0.26	1.79 ± 0.35
059/01	7.79	2.57 ± 0.61	2.51 ± 0.61	2.99 ± 0.66	2.49 ± 0.36	2.35 ± 0.45
085/03	1.27	3.01 ± 0.40	3.3 ± 0.40*	5.75 ± 0.66	2.36 ± 0.28	0.96 ± 0.33
146/01	15.26	3.94 ± 0.55	3.85 ± 0.55	2.12 ± 0.65	2.49 ± 0.37	1.26 ± 0.41
170/01	8.92	-1.29 ± 0.54	-1.32 ± 0.54	3.12 ± 0.66	2.48 ± 0.56	3.55 ± 0.63
196/02	30	3.17 ± 0.67	3.03 ± 0.67	2.39 ± 0.71	2.58 ± 0.40	2.24 ± 0.46
2002/01-2016/12						
185/01	24.81	3.77 ± 0.55	3.68 ± 0.55	3.74 ± 0.77	4.26 ± 0.54	3.78 ± 0.52
2002/01-2015/12						
044/02	11.70	3.29 ± 0.62	3.38 ± 0.62	3.45 ± 0.94	3.47 ± 0.41	2.36 ± 0.42
085/01	9.93	4.40 ± 0.79	4.37 ± 0.79	4.21 ± 0.70	4.20 ± 0.39	2.48 ± 0.47
085/04	10.73	4.20 ± 0.64	4.50 ± 0.64	1.38 ± 0.57	1.82 ± 0.38	-0.67 ± 0.40
085/05	28.65	4.20 ± 0.64	4.50 ± 0.64	5.06 ± 0.70	2.04 ± 0.38	-0.75 ± 0.41
109/03	17.37	4.18 ± 0.92	4.12 ± 0.92	3.56 ± 1.01	4.24 ± 0.65	3.88 ± 0.65
196/04	14.43	7.95 ± 0.77	7.97 ± 0.77	4.08 ± 0.80	4.51 ± 0.43	2.84 ± 0.48
222/02	25.75	4.20 ± 0.64	4.50 ± 0.64	0.42 ± 0.65	2.32 ± 0.36	-0.55 ± 0.41

We note some general agreement in terms of trend between the different SLA and TG within the respective uncertainties (for example, for sites 059/01, 146/1, 196/2, 185/01, 44/2, 85/1, 85/5 and 109/3). We also observe good agreement between the coastal SLA trends and the gridded CMEMS/DT2018 trends, except for 85/3 (Senetosa site). In the latter case, the discrepancy was previously discussed in Gouzenes et al. (2020) and attributed to physical processes acting close to the coast (see also next section), thus not seen by the gridded products of about $\frac{1}{4}^\circ$ resolution. A similar discrepancy can be observed for tracks 85/5 and 222/2. We cannot exclude that in these cases too, some local factors either affect the tide gauge (e.g., a local VLM superimposed to the GIA, and not accounted for here) or the points on the Jason track (e.g., local ocean dynamic variations not seen by the tide gauge).

As for the correlation at interannual time scale (Table 2), no clear relationship is observed between trend differences and distance between tide gauge and Jason track. Finally, concerning the CMEMS Med-Physics model based trends, the agreement with the altimetry trends is poor for most of the sites (except 59/1, 196/2 and 109/3).

4. The case of the Senetosa site (Jason track 085/03)

In this section, we focus on the Senetosa site (track 085/03), the calibration site for the Topex/Poseidon and Jason altimetry missions. Recently, Gouzenes et al. (2020) showed that, over the June 2002-May 2018 time span, the sea level trend at Senetosa increases as the distance to the coast decreases. Gouzenes et al. (2020) showed that the trend increase in the last 3-4 km to the coast could not be explained either by erroneous trends in the geophysical corrections (i.e. sea state bias, wet tropospheric correction, dynamic atmospheric correction, ocean tide and ocean loading tide) applied to the altimetry data or by errors in the ALES retracking (use of the standard MLE4 retracker of Jason altimeter missions leads to the same trend behavior). They concluded that some small-scale physical process may be responsible for the observed trend increase (see for example Woodworth et al., 2019). They evaluated the contribution of waves but concluded that trend in waves is too small and active too close to the coast (last 1 km) to explain the reported trend increase.

In the present study, we examine another potential coastal process, i.e., the effect of sea water temperature T and salinity S changes close to the coast. Because of the lack of in situ ocean parameters measurements, we use high-resolution data from the MARS3D model, available over January 2014-December 2019 (unfortunately, the model output are not available prior January 2014). We interpolated the model T/S data along the 085/03 Jason track and computed the T/S trends as a function of depth and distance to the coast. Corresponding 2-dimensional T & S maps are shown in Fig.3a and Fig.3b. We note an increase of the temperature trend with depth as the distance to the coast decreases. This indicates a thermocline deepening close to the coast (Fig.3a). An opposite effect is observed for the salinity trend with a decrease in salinity close to the coast (Fig.4b). These physical characteristics (increasing temperature trends and decreasing salinity trends) occur in the last ~ 4 km to the coast and are highly correlated with the bathymetry (see Fig.3a, 3b).

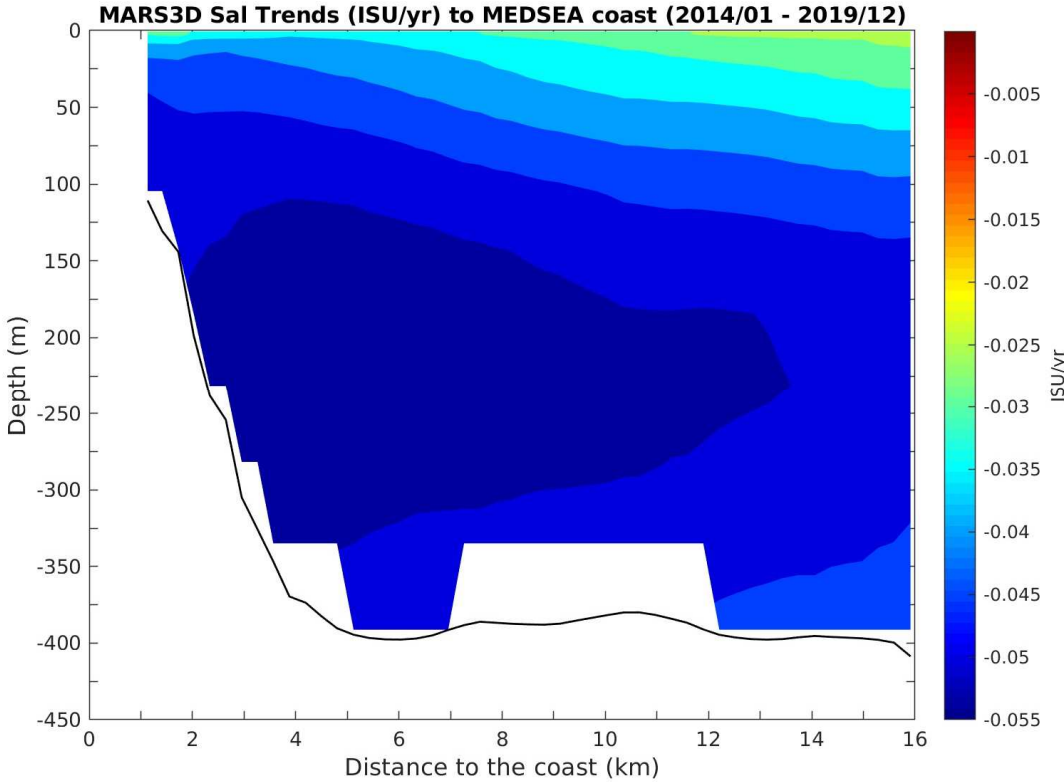
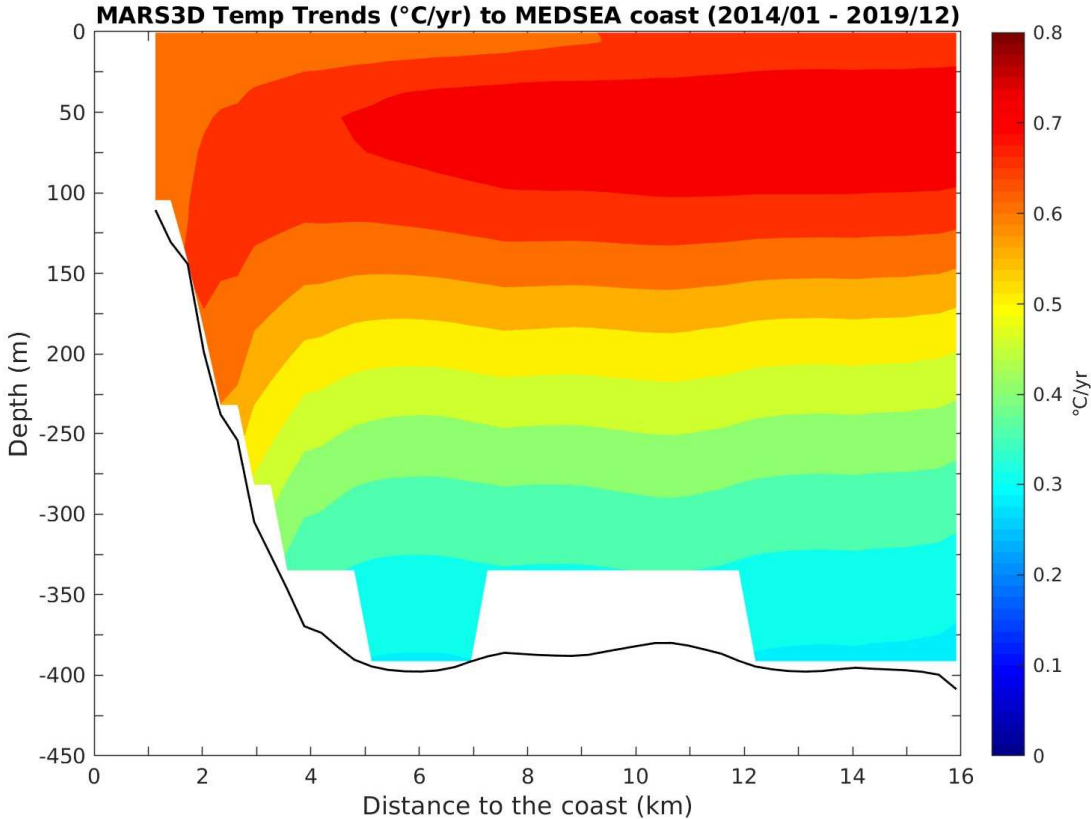


Fig. 3: (a) Temperature trend map, for site 085/03 near Senetosa. Based on the MARS3D

model (calculated over the period January 2014 – December 2019) as a function of depth and distance at the coast along the altimeter track over the first 16 km of the coast. (b) same as (a) but for the salinity. The black curve is the bathymetric profile from the MARS3D model.

We further computed separately the along-track thermosteric (T effect) and halosteric (S effect), integrating T/S data down to the seafloor:

$$H = H_T + H_S = \int_0^z \alpha (T - T_0) dz + \int_0^z \beta (S - S_0) dz \quad (1)$$

With H: steric sea level, H_T : thermosteric sea level, H_S : halosteric sea level, $T - T_0$: temperature anomaly, $S - S_0$: salinity anomaly. z is integration depth (integration between surface and seafloor); α and β are coefficients of thermal and haline expansion.

Fig.4 shows the thermosteric and halosteric sea level trends against distance to the coast, as well as their sum (steric component). The altimetry-based coastal sea level trend (over 2002-2019) is also superimposed.

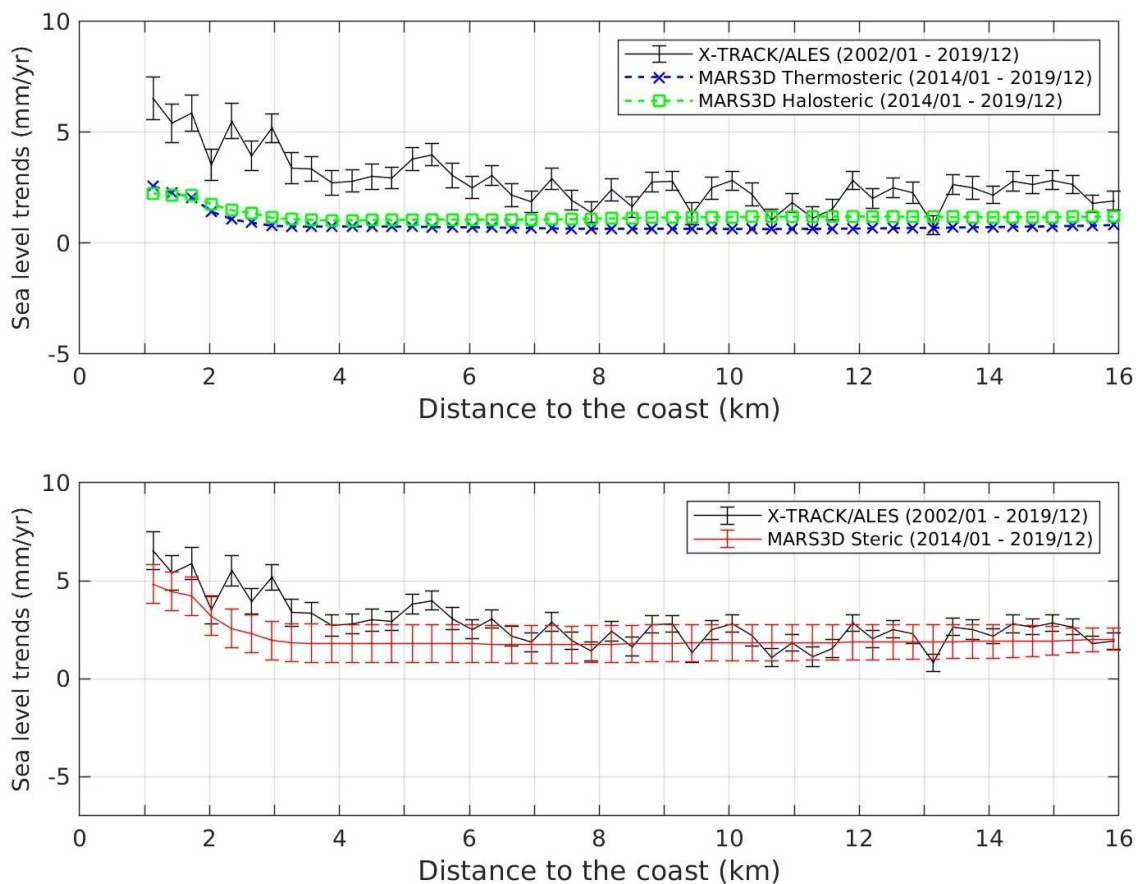


Fig. 4. Upper panel: SLA trends at Senetos a (calculated over the period January 2002 -

December 2019) (black curve) against distance to the coast compared to the thermosteric and halosteric trends (green and blue curves respectively). Lower panel: same as upper panel but with the total steric trends (red curve)

Although observed and modeled coastal trends are not estimated over the same time span their respective behaviours against distance to the coast are very similar. Unfortunately, we cannot estimate reliable SLA trends over a time span as short as 6 years, i.e., 2014-2019, the results being too noisy as illustrated in Fig.5 showing coastal SLA trend errors as a function of record length.

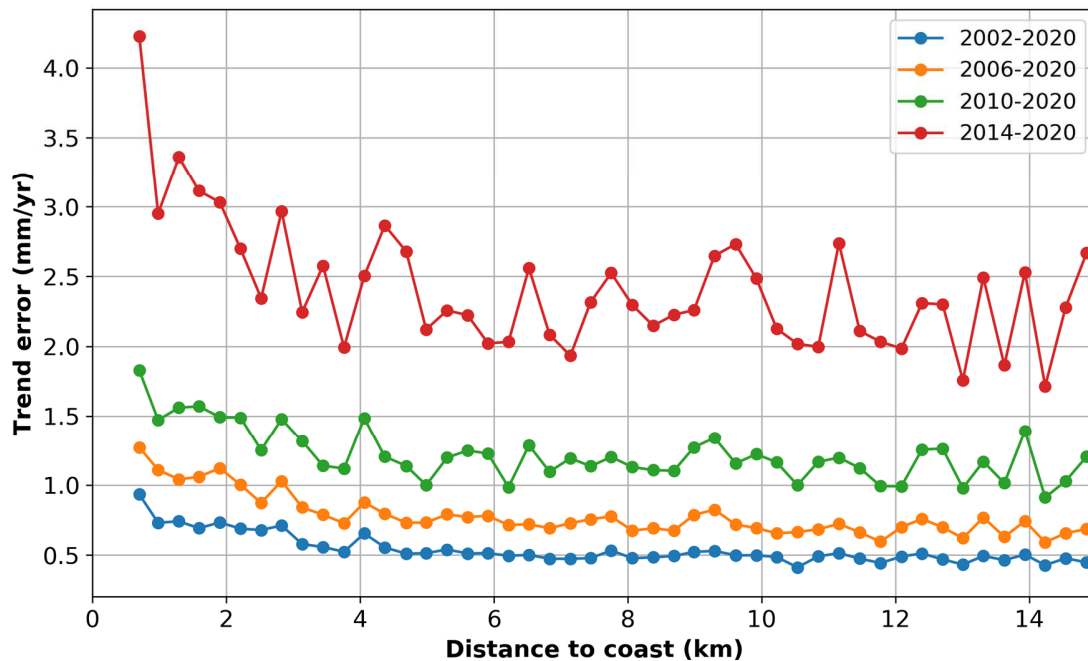


Fig.5: SLA trend errors against distance to the coast for different record length.

This good agreement observed in Fig.3b between SLA and steric trends may be fortuitous. Hence, the only conclusion we can draw so far is that, if the steric trend behaviour is a long-lived feature, change in T/S nearby Senetosa may be invoked to explain the SLA trend increase towards the coast. This could be eventually related to the presence of a wind-driven small-scale coastal current nearby the Senetosa shoreline, as shown in Gouzenes et al. (2020).

Fig. 6 shows SLAs trends and bathymetric profiles against distance to the coast for two different data sources: ETOPO2v2c_f4 (NOAA, 2006; <https://www.ngdc.noaa.gov/mgg/bathymetry/relief.html>) and the MARS3D model. Several publications have already highlighted a possible impact of bathymetry on water height variations using geophysical circulation and geomorphology models (Huthnance, 1987; Wise et al., 2018). The observed seafloor depth decrease close to the Senetosa coast may influence the sea water density distribution (i.e., the isopycnal lines), with a direct impact on the steric trend increase. Lazure and Dumas (2008) showed that in shallow coastal areas, the dynamics of the thermal and haline structure of the upper ocean is quite complex due to the spatial and temporal variability of wind stress

and heat fluxes. The latter induce turbulent mixing that causes temperature and salinity variations within the surface layers and consequently, density stratification.

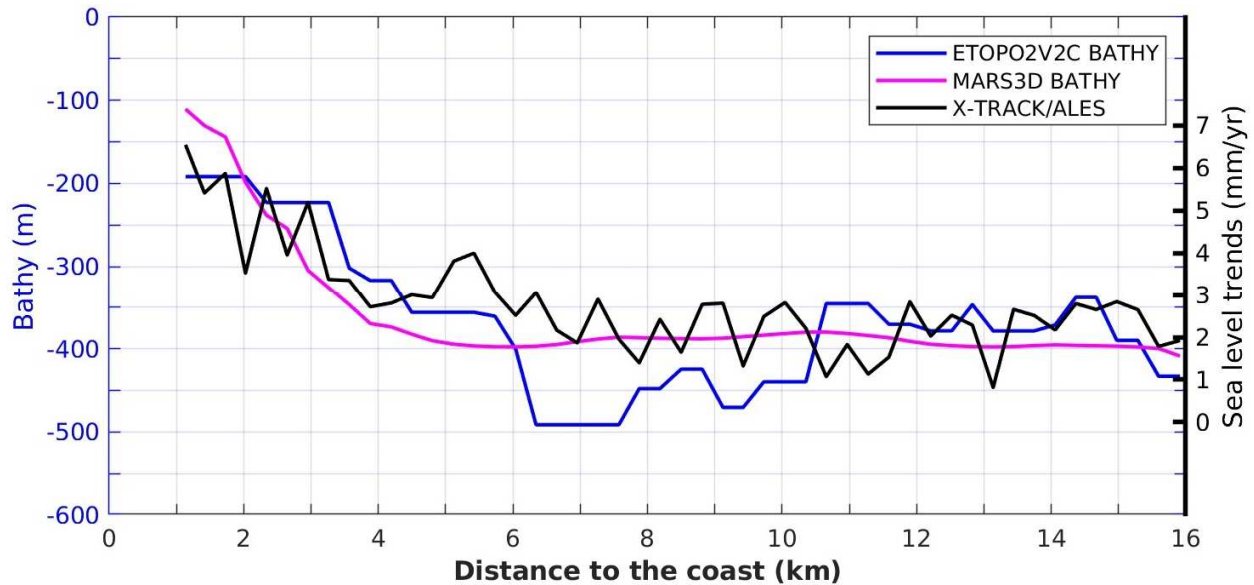


Fig.6. SLA trends with bathymetric profile superimposed (from two sources: ETOPO2v2c_f4 and the MARS3D model).

6. Summary and conclusion

The validation of X-TRACK/ALES SLA trends is important because it contributes to answer the question: is the SLA trend at the coast similar to offshore? If a difference is observed (after appropriate validation), the next question is: what are the coastal physical processes causing such a difference? The answer to this question is important, not only for the consequences on coastal populations, but also because past reconstructions of global mean sea level are based on sea level measurements at the coast by tide gauges. Therefore, differences in coastal - offshore trends may affect past sea level reconstructions and inferred GMSL rate of rise.

The present study has allowed to validate the 20 Hz altimetry data from X-TRACK/ALES product in the Mediterranean Sea by comparing with tide gauge records at a few selected sites. In terms of interannual variability the agreement between coastal SLA and TG time series is good with a correlation generally > 0.7 . The altimetry-TG trend comparison shows general agreement, except at a few sites where local factors may be different at the tide gauge site and along the Jason track.

Our investigation of the steric contribution to sea level at Senetosa using the high-resolution MARS3D model suggests a direct impact of T/S changes close to the coast influenced by the bathymetry.

The effects of small-scale coastal processes on sea level near the coast remain to be determined on a more general basis. Availability of in situ data (e.g., T/S, currents) as well as very high resolution (< 1 km) numerical models with records available over a fairly long period (>15 years) over the entire Mediterranean Sea are currently lacking. Efforts to extend in situ coastal networks with sustained observing systems, as well as to develop high-resolution numerical models over more than a few years are strongly recommended.

Acknowledgements

H.B. Dieng was supported by an OCEANEXT contract. Yvan Gouzenes is supported by a grant (reference 4000126561/19/I-NB) from the European Space Agency in the context of the Climate Change Initiative (CCI) Coastal Sea Level project. We thank three anonymous reviewers for their constructive comments that helped us to improve the manuscript.

References

- Angnuureng, D.B., Appeaning, Addo K., Almar, R., Dieng, H.B., 2018. Influence of sea level variability on a micro-tidal beach. *Nat. Hazards* 93 (3), 1611–1628. <https://doi.org/10.1007/s11069-018-3370-4>.
- Birol F., N.X Fuller, F. Lyard, et al., (2017). Coastal applications from nadir altimetry: example of the X-TRACK regional products. *Advances in Space Research*, 59, 936-953, <https://doi.org/10.1016/j.asr.2016.11.005>.
- Birol F., F. Léger, M. Passaro, A. Cazenave, F. Niño, F. Callafat, A. Shaw, J.-F. Legeais, Y. Gouzenes, C. Schwatke and J. Benveniste, 2021. The X-TRACK/ALES multi-mission processing system: new advances in altimetry towards the coast. *Advances in Space Research*, in press.
- Bonnefond, P., Haines, B., and Watson, C., 2011. In Situ Calibration and Validation: A Link from Coastal to Open-ocean altimetry, in: *Coastal Altimetry*, Chapt. 11, pp. 259–296, edited by: Vignudelli, S., Kostianoy, A., Cipollini, P., Benveniste, J., Springer, Berlin, ISBN: 978-3-642-12795-3, https://doi.org/10.1007/978-3-642-12796-0_11.
- Church, J. A., Clark, P. U., Cazenave, A., et al., 2013, 'Sea level change', in: Stocker, T. F., Qin, D., Plattner, G.-K., et al. (eds), *Climate change 2013: The physical science basis. Contribution of Working Group I to the Fifth Assessment Report of the Intergovernmental Panel on Climate Change*, Cambridge University Press, Cambridge; New York, pp. 1137–1216.
- Cipollini, P., Calafat, F.M., Jevrejeva, S., Melet, A., Prandi, P., 2017. Monitoring Sea Level in the Coastal Zone with Satellite Altimetry and Tide Gauges. *Surv. Geophys.* 38 (1), 33–57. <https://doi.org/10.1007/s10712-016-9392-0>.
- Dangendorf, S, Marcos M., Wöppelmann G. , Clinton C.P., Frederikse T. , and Riccardo Riva R., 2017. “Reassessment of 20th Century Global Mean Sea Level Rise.” *Proceedings of the National Academy of Sciences* 114 (23):5946–51. <https://doi.org/10.1073/pnas.1616007114>.
- Dee, D. P., S. M. Uppala, A. J. Simmons, P. Berrisford, P. Poli, S. Kobayashi, U. Andrae et al., 2011. "The ERA-Interim reanalysis: Configuration and performance of the data assimilation system". *Quarterly Journal of the Royal Meteorological Society*, 137, 656, 553-597.
- Deng Z., Gendt G., Schöne T., 2015. Status of the IGS-TIGA Tide Gauge Data Reprocessing at GFZ. In: Rizos C., Willis P. (eds) *IAG 150 Years. International Association of Geodesy Symposia*, vol 143. Springer, Cham https://link.springer.com/chapter/10.1007%2F1345_2015_156.

- Dieng H. B., Dadou I., Léger F. et al., 2019. Sea level anomalies using altimetry, model and tide gauges along the African coasts in the Eastern Tropical Atlantic Ocean: Inter-comparison and temporal variability. *Advances in Space Research*, <https://doi.org/10.1016/j.asr.2019.10.019>.
- Gouzenes Y., Léger F., Cazenave A., Birol F., Bonnefond P., Passaro M., Nino F., Almar A., Laurain O., Schwatke C., Legeais J-F. and Benveniste J. (2020). Coastal sea level rise at Senetosa (Corsica) during the Jason altimetry missions. *Ocean Sci.*, 16, 1165–1182, 2020 <https://doi.org/10.5194/os-16-1165-2020>.
- Gómez-Enri, J., Vignudelli, S., Cipollini, P., Coca, J., Gonzalez, C.J., 2018. Validation of CryoSat-2 SIRAL sea level data in the Eastern continental shelf of the Gulf of Cadiz. *Adv. Space Res.* 62 (6), 1405–1420. <https://doi.org/10.1016/j.asr.2017.10.042>.
- Grgić, M., Nerem, R.S. and Bašić, T., 2017. Absolute sea level surface modeling for the Mediterranean from satellite altimeter and tide gauge measurements, *Mar. Geod.*, 40 (4), 239–258. <https://doi.org/10.1080/01490419.2017.1342726>.
- Holgate, S.J.; Matthews, A.; Woodworth, P.L.; Rickards, L.J.; Tamisiea, M.E.; Bradshaw, E.; Foden, P.R.; Gordon, K.M.; Jevrejeva, S., and Pugh, J., 2013. New data systems and products at the Permanent Service for Mean Sea Level. *Journal of Coastal Research* (2013) 29 (3): 493–504. doi.org/10.2112/JCOASTRES-D-12-00175.1.
- Huthnance J.M., 1987. Along-shelf evolution and sea levels across the continental slope. *Continental Shelf Research*, 7, 8, 957-974, ISSN 0278-4343, [https://doi.org/10.1016/0278-4343\(87\)90008-2](https://doi.org/10.1016/0278-4343(87)90008-2).
- Idris, N.H., Deng, X., Din, A.H.Md., Idris, N.H., 2017. CAWRES: a waveform retracking fuzzy expert system for optimizing coastal sea levels from Jason-1 and Jason-2 Satellite Altimetry Data. *Remote Sens.* 9 (6), 603, doi: 10.3390/rs9060603.
- Lazure P and Dumas F., 2008. [An external-internal mode coupling for a 3D hydrodynamical model for applications at regional scale (MARS). *Adv. Water Resour.*, 31, 233–250.
- Legeais J.F., Ablain M., Zawadzki L. et al., 2018. An improved and homogeneous altimeter sea level record from the ESA Climate Change Initiative, *Earth Syst. Sci. Data*, 10, 281-301, <https://doi.org/10.5194/essd-10-281-2018>.
- Marti F., Cazenave A., Birol F., Passaro, M. Leger F., Nino F., Almar R., Benveniste J. and Legeais J.F., 2019. Altimetry-based sea level trends along the coasts of western Africa. *Advances in Space Research*, <https://doi.org/10.1016/j.asr.2019.05.033>.
- NOAA National Geophysical Data Center. 2006. 2-minute Gridded Global Relief Data (ETOPO2) v2. NOAA National Centers for Environmental Information. <https://doi.org/10.7289/V5J1012Q>. Accessed [2020].
- Oddo P., M. Adani N. Pinardi, C. Fratianni, M. Tonani, D. Pettenuzzo, 2009. A Nested Atlantic-Mediterranean Sea General Circulation Model for Operational Forecasting. *Ocean Sci. Discuss.*, 6, 1093-1127.
- Passaro, M., Cipollini, P., Vignudelli, S., Quartly, G. D., & Snaith, H. M., 2014. ALES: A multi-mission adaptive subwaveform retracker for coastal and open ocean altimetry. *Remote Sensing of Environment*, 145, 173-189.
- Peltier W.R., 2004. Global Glacial Isostasy and the Surface of the Ice-Age Earth: The ICE-5G(VM2) model and GRACE. *Ann. Rev. Earth. Planet. Sci.* 2004. 32,111-149.
- Peng, F. and Deng, X., 2018. Validation of improved significant wave heights from the Brown-Peaky (BP) Retracker along the East Coast of Australia. *Remote Sens.* 10, 7, 1072[19 p.], doi: 10.3390/rs10071072.
- Risien, C.M. and Strub, P.T., 2016. Blended sea level anomaly fields with enhanced coastal coverage along the U.S. West Coast. *Nature Scientific data*, 3, 160013, doi: 10.1038/sdata.2016.13.

- Ruiz Etcheverry, L.A., Saraceno, M., Piola, A.R., Valladeau, G., Möller, O.O., 2015. A comparison of the annual cycle of sea level in coastal areas from gridded satellite altimetry and tide gauges. *Continental Shelf Res.*, 92, 1, 87–97, doi: 10.1016/j.csr.2014.10.006.
- Salazar-Ceciliano, J., Trasviña-Castro, A., González-Rodríguez, E., 2018. Coastal currents in the Eastern Gulf of Tehuantepec from coastal altimetry. *Adv. Space Res.* 62 (4), 866–873. <https://doi.org/10.1016/j.asr.2018.05.033>.
- Simoncelli, S., Fratianni, C., Pinardi, N., Grandi, A., Drudi, M., Oddo, P., & Dobricic, S., 2019. Mediterranean Sea Physical Reanalysis (CMEMS MED-Physics) [Data set]. Copernicus Monitoring Environment Marine Service (CMEMS). https://doi.org/10.25423/MEDSEA_REANALYSIS_PHYS_006_004.
- Taburet, G., Sanchez-Roman, A., Ballarotta, M., Pujol, M.I., Legeais, J.-F., Fournier, F., Faugere, Y., Dibarboure, G., 2019. DUACS DT-2018: 25 years of reprocessed sea level altimeter products. *Ocean Sci.* 15 (5), 1207–1224. <https://doi.org/10.5194/os-15-1207-2019>.
- The Climate Change Coastal Sea Level Team (2020). A database of coastal sea level anomalies and associated trends from Jason satellite altimetry from 2002 to 2018. SEANOE. <https://doi.org/10.17882/74354>.
- Valladeau G., P. Thibaut, B. Picard, J. C. Poisson, N. Tran, N. Picot & A. Guillot, 2015. Using SARAL/AltiKa to Improve Ka-band Altimeter Measurements for Coastal Zones, Hydrology and Ice: The PEACHI Prototype. *Marine Geodesy*, 38:sup1, 124-142, DOI:10.1080/01490419.2015.1020176.
- Watson, C. S., N. J. White, J. A. Church, M. A. King, R. J. Burgette, and B. Legresy, 2015. Unabated global mean sea level over the satellite altimeter era, *Nat. Clim. Change*, doi:10.1038/NCLIMATE2635.
- Wise A., Hughes C.W, and Polton J.A., 2018. Bathymetric Influence on the Coastal Sea Level Response to Ocean Gyres at Western Boundaries, *Journal of Physical Oceanography*, 48 (12), 2949–2964 <https://doi.org/10.1175/JPO-D-18-0007.1>
- Woodworth, P.L., Melet, A., Marcos, M., Ray, R.D., Wöppelmann, G., Sasaki, Y.N., Cirano, M., Hibbert, A., Huthnance, J.M., Monserrat, S., Merrifield, M.A., 2019. Forcing factors affecting sea level changes at the coast. *Surv. Geophys.*, 1–47 <https://doi.org/10.1007/s10712-019-09531-1>, ISSN 1573-095.